Adaptive Restoration of Speckled SAR Images Using a Compound Random Markov Field

José M. B. Dias, Tiago A. M. Silva, and José M. N. Leitão
Instituto Superior Técnico
Departamento de Engenharia Electrotécnica e de Computadores, and
Instituto de Telecomunicações
Tel: +351 1 8418466; Fax: +351 1 8418472; E-mail: bioucas@lx.it.pt

Abstract

This paper proposes a restoration scheme for noisy images generated by coherent imaging systems (e.g., synthetic aperture radar, synthetic aperture sonar, ultrasound imaging, and laser imaging). The approach is Bayesian: the observed image intensity is assumed to be a random variable with gamma density; the image to be restored (mean amplitude) is modeled by a compound Gauss-Markov random field *which enforces smoothness on homogeneous regions while preserving discontinuities between neighboring regions. A Neyman-Pearson detection criterion is used to infer the discontinuities, thus allowing to select a given false alarm probability maximizing the detection probability. The whole restoration scheme is then cast into a* maximum a posteriori probability *(MAP) problem. An* expectation maximization *type iterative scheme embedded in a continuation algorithm is used to compute the MAP solution. An application example performed on radar data is presented.*

I. Introduction

Coherent imaging systems are designed aiming at the acquisition of the scene *complex reflectivity*. They are linear systems whose output is given by the convolution between its coherent *point spread function* (PSF) and the scene complex reflectivity. Examples are *synthetic aperture radar* (SAR), *synthetic aperture sonar* (SAS), *ultrasound imaging*, and laser imaging. The complex reflectivity originated in a given *resolution cell* is composed by the contributions of all individual scatterers lying in that cell. These contributions interfere randomly in a destructive or constructive manner, according to the spatial configuration of the scatterers. This random fluctuation is termed (*speckle noise*); its statistical properties have been addressed in several references [1], [2], [3]. Assuming that the surface being illuminated is rough compared to the wavelength, that there are no strong specular reflectors, and that there is a large number of scatterers per resolution cell, then the squared amplitude (*intensity*) of the complex reflectivity is exponentially distributed; the scenario just described, termed *fully developed speckle*, leads to highly noisy intensity images: the *signal to noise ratio* (SNR), defined as the square of the ratio between the intensity mean value (backscatering coefficient) and the intensity variance, is one. The granular appearance of intensity images is due to this very low SNR.

This work was supported by Portuguese PRAXIS XXI program, under project 2/2.1.TIT/1580/95

Most applications involving coherent systems data rely on the mean intensity image (backscattering coefficient image). In view of the rationale above presented, there is need for applying speckle reduction/restoration techniques to intensity data. A common approach consists in averaging independent observations of the same pixel, which in the case of SAR systems is called *multi-look*. This term stems from the fact that each independent sample is generated by a different segment of the SAR array. Independently of the system, an image formed by the averaging of m independent samples will herein be termed an *m-look* image. For fully developed speckle, the SNR of an *m-look* image is m. However, increasing the number of independent samples results in reduction of spatial resolution, being necessary to resort to spatial smoothing techniques. The basic idea underlying these techniques is that of applying nonuniform smoothness in such a way that homogeneous image regions, in a statistical sense, are highly smooth, while discontinuities are preserved [4], [5], [6].

In recent years a significant research activity has been devoted to the development of speckle reduction techniques, or, equivalently, to the mean backscattering coefficient estimation. These techniques take the form of image restoration [7], [8], edge detection [9], or image segmentation algorithms [3], [10], [11], [12], [13]. A common assumption is that images are locally smooth. This behavior has been modeled mainly by *ad hoc* techniques [7], or by *Markov random fields* [3], [10], [11], [12].

The present approach is Bayesian:

- the observed image, given the backscattering coefficients, is assumed to be a realization of a random field taking into account the statistics of image reflectivity;
- the set of backscattering coefficients associated to the image pixels is assumed to be *piecewise smooth*, and modeled as a random field with a *compound Gauss-Markov random field* (CGMRF) prior [5], [14].

The piecewise smoothness assumption makes sense in many situations: e.g., SAR images of agricultural landscapes, echography of the human body, etc.

The methodology herein proposed is on the vein of work

[15]. Its main contribution is on a new approach to the line field discontinuity dectection; the Neyman-Pearson detection criterion is used, thus allowing to select a given false alarm probability maximizing the detection probability.

II. Proposed Approach

Assume that images are defined on the $N \times N$ rectangular lattice $Z_N = \{(i,j), i,j = 1,\ldots,N\}$. Define $\mathbf{F} = \{F_{ij}\}$ and $\mathbf{G} = \{G_{ij}\}$, with $(i,j) \in Z_N$ as the random fields associated to the square root of the backscattering coefficient image and the observed intensity image, respectively. Lowercase letters will denote the values assumed by the the random fields as well as its realizations.

Besides fields $\mathbf{F}$ and $\mathbf{G}$, it is assumed the existence of another field, $\mathbf{L} = \{\mathbf{H}, \mathbf{V}\}$, with $\mathbf{H} = \{H_{ij}\}$ and $\mathbf{V} = \{V_{ij}\}$, signaling horizontal and vertical discontinuities. Variables V_{ij} and H_{ij} are binary, taking value 1 if a discontinuity is present and 0 otherwise. The field $\mathbf{L}$, also termed *line field* [5], serves the purpose of avoiding edges to be smoothed out during the restoration of field $\mathbf{F}$.

For compactness, the probability density of the generic field $\mathbf{X}$, $p_{\mathbf{x}}(\mathbf{X} = \mathbf{x})$, or of the generic random variable X, $p_x(X = x)$, will be denoted by $p(\mathbf{x})$ and $p(x)$, respectively. For example, the density $p_{FL|G}(\mathbf{F} = \mathbf{f}, \mathbf{L} = \mathbf{l}|\mathbf{G} = \mathbf{g})$, will be denoted as $p(\mathbf{f}, \mathbf{l}|\mathbf{g})$.

A. Image Generation Mechanism

Under the fully developed speckle hypothesis, the complex amplitude $x = x_r + jx_i$ (inphase and quadrature components) of the backscattered field, at each pixel, is circularly symmetric and Gaussian [10]. Thus

$$p(x|f) = \frac{1}{\pi f^2} e^{-\frac{|x|^2}{f^2}}, \tag{1}$$

where $f^2 := E[|x|^2]$ is the backscattering coefficient of the referred resolution cell. For intensity or power images the data is in the form of square magnitude of the complex components, $g = |x|^2$. Random variable G is therefore the exponentially distributed:

$$p(g|f) = \frac{1}{f^2} e^{-\frac{g}{f^2}}. \tag{2}$$

For an m-look image, G is the average of m independent exponentially distributed random variables, thus having gamma density [16],

$$p(g|f) = \frac{1}{\Gamma(M)} \left(\frac{f^2}{M}\right)^{-M} g^{M-1} \exp\left(-\frac{gM}{f^2}\right), \tag{3}$$

with $E[g|f] = f^2$ and $\sigma^2[g|f] = f^2/M$.

It is herein assumed that the components of $\mathbf{g}$, given $\mathbf{f}$, are independent. Hence

$$p(\mathbf{g}|\mathbf{f}) = \prod_{ij \in Z_N} p(g_{ij}|f_{ij}). \tag{4}$$

The conditional independence assumption is valid if the resolution cells associated to any pair of pixels are disjoint. This is only true if the size of the imaging system PSF is smaller than the corresponding interpixel distance. This is approximately true in most acquisition systems. Otherwise, neighboring data would be extremely correlated, adding no information.

B. Prior Model

Image $\mathbf{f}$ is assumed to be *piecewise smooth*. This makes sense whenever the scene is made of smooth regions, concerning the backscattering coefficient. *Gauss-Markov random fields* [17] are both mathematically and computationally suitable for representing local interactions, particularly continuity between neighboring pixels. However, the continuity constraint must be discarded for those sites near the discontinuities. For this purpose we take the *first order* noncausal CGMRF

$$p(\mathbf{f}|\boldsymbol{l}) = \frac{1}{Z_1(\mathbf{l})} e^{-2\mu \sum_{ij} \omega(\Delta^h_{ij})^2 \bar{v}_{ij} + \omega(\Delta^v_{ij})^2 \bar{h}_{ij} + (1-4\omega)) f^2_{ij}}, \tag{5}$$

where $\bar{v}_{ij} := (1 - v_{ij})$, $\bar{h}_{ij} := (1 - h_{ij})$, $\Delta^h_{ij} := (f_{ij} - f_{i,j-1})$, $\Delta^v_{ij} := (f_{ij} - f_{i-1,j})$, $Z_1(\mathbf{l})$ is the so-called *partition function* and $(2\mu\omega)^{-1}$ has the meaning of the variance of the increments Δ^h_{ij} and Δ^v_{ij}. Notice that continuity constraint between sites (i,j) and $(i,j-1)$ is removed if variable v_{ij} is set to one; the same is true concerning sites (i,j), $(i-1,j)$ and horizontal line h_{ij}.

Parameter ω plays only a tecnical role in assuring that density (5) is valid, and should be chosen so as to $\omega < 1/4$; note that for values of ω very close to $1/4$ the third term of (5) affects very little $p(\boldsymbol{f}|\boldsymbol{l})$, yet leads to an integrable density.

C. Density Distribution Given the Line Field

Invoking the Bayes rule, and noting that $p(\mathbf{g}|\mathbf{f}, \mathbf{l}) = p(\mathbf{g}|\mathbf{f})$, we obtain the joint probability density function of $(\mathbf{f}, \mathbf{g})$, given $\mathbf{l}$, as

$$p(\mathbf{f}, \mathbf{g}|\mathbf{l}) = p(\mathbf{g}|\mathbf{f}) p(\mathbf{f}|\mathbf{l}). \tag{6}$$

Replacing expressions (3) and (5) in (6), the joint density of $(\mathbf{f}, \mathbf{g})$, conditioned on $\mathbf{l}$, is then given by

$$p(\mathbf{f}, \mathbf{g}|\mathbf{l}) = \frac{1}{Z_2} e^{-U(\mathbf{f}, \mathbf{g}|\mathbf{l})}, \tag{7}$$

where

$$-U(\mathbf{f}, \mathbf{g}|\mathbf{l}) = \tag{8}$$

$$- \quad 2M \log f_{ij} - \frac{M g_{ij}}{f^2_{ij}}$$

$$- \quad 2\mu \sum_{ij} \omega \bar{v}_{ij} (\Delta^h_{ij})^2 + \omega \bar{h}_{ij} (\Delta^v_{ij})^2 + (1 - 4\omega) f^2_{ij}$$

$$- \quad \log Z_1(\mathbf{l}) + c^{te}. \tag{9}$$

III. The Line Field

The line field $\mathbf{l}$ is not known and has to be estimated from the observed data $\mathbf{g}$. The first thought that comes to mind is the *maximum likelihood* (ML) estimate $\widehat{\mathbf{l}}_{ML}$. The ML solution is however useless since it gives $\hat{h}_{ij} = \hat{v}_{ij} = 1$ everywhere, besides the unberable complexity in computing the partition function $Z(\mathbf{l})$ [18].

To cope with the difficulties of the ML estimate, it is necessary to penalize somehow the creation of discontinuities. This can be done by assuming that images $\mathbf{f}$, $\mathbf{l}$ are both random field with a given prior $p(\mathbf{f}, \mathbf{l})$. This strategy, or an equivalent one, has been folowed, for example, in [4], [5], [6]. Work [18] proposes a penalizing term based on an *information theoretical* viewpoint; this approach is however equivalent to the Bayesian one.

In this paper we address the line field estimation from a *detection theory* point of view. The basic ideia is to design a *binary decision rule* that, based on the observed differences Δ^h_{ij}, should decide:
1. H_0: discontinuity is not present ($v_{ij} = 0$);
2. H_1: discontinuity is present ($v_{ij} = 1$).

The same binary decision rule should apply also to Δ^v_{ij}.

Fundamental components of a decision problem are the conditional probabilities densities $p(\Delta^h_{ij}|H_0)$ and $p(\Delta^h_{ij}|H_0)$ (the so-called *probabilistic transition mechanism*); given the multidimensional Gaussian density (5), we have

$$p(\Delta_{ij}|H^h_0) = \frac{1}{\sqrt{2\pi}\sigma_0} e^{-\frac{\Delta^2}{2\sigma_0^2}} \quad (10)$$

$$p(\Delta_{ij}|H^h_1) = \frac{1}{\sqrt{2\pi}\sigma_1} e^{-\frac{\Delta^2}{2\sigma_1^2}}, \quad (11)$$

where σ_0 and σ_1 are functions of $\mathbf{l}$ and ω. For $\omega \simeq 1/4$, we have $\sigma_0^2 \simeq \mu^{-1}$. The lowest value that σ_1 can take is $\sigma_1^2 = (\mu(1-4\omega))^{-1}$, when all the four discontinuities between site (ij) and its neighbors are signaled. Notice that $\sigma_1^2 \gg \sigma_0^2$ since $\omega \simeq 1/4$.

Since priors $p(H_0)$ and $p(H_1)$ are unknown, we derive the decision rule based on the *Neyman-Pearson* criterion [19]. For the problem at hands, it can be shown that the Neyman-Pearson criterion leads to the decision rule

$$\widehat{v}_{ij} = \max_{v_{ij}\in\{0,1\}} \left(-(\Delta^h_{ij})^2 - \alpha v_{ij}\right) \quad (12)$$

where, for the false alarm probability P_F,

$$\alpha \simeq 2\frac{\sigma_0^2\sigma_1^2}{\sigma_1^2 - \sigma_0^2} \log \frac{1}{P_F}. \quad (13)$$

For $\sigma_1 \gg \sigma_0$, the treshold (13) is, approximately, given by $\alpha = 2\sigma_0^2 \log P_F^{-1}$, hence, independent of σ_1.

Although we have not dealt with $\mathbf{l}$ as a random field, it is convinent to introduce the following prior

$$p(\mathbf{l}) = \frac{Z_1(\mathbf{l})}{Z_3} e^{-\alpha\|\mathbf{l}\|}. \quad (14)$$

The joint probability $p(\mathbf{f}, \mathbf{l}) = p(\mathbf{f}|\mathbf{l})p(\mathbf{l})$ is than given by

$$p(\mathbf{f}, \boldsymbol{l}) = \frac{1}{Z} e^{-2\mu \sum_{ij} \omega(\Delta^h_{ij})^2 \bar{v}_{ij} + \omega(\Delta^v_{ij})^2 \bar{h}_{ij} + (1-4\omega))f^2_{ij} - 2\mu\omega\alpha\|\mathbf{l}\|}. \quad (15)$$

We now note that, for a given $\mathbf{f}$, the solution of

$$\widehat{\mathbf{l}} = \arg\max_{\mathbf{l}} p(\mathbf{f}, \boldsymbol{l}) \quad (16)$$

is $\widehat{\mathbf{l}} = \{\widehat{v}_{ij}, \widehat{h}_{ij}\}$, where $\widehat{v}_{ij}$ is given by (12), and $\widehat{h}_{ij}$ likewise replacing v with h.

To jointly estimate field $\mathbf{f}$ and $\mathbf{l}$, we adpot the follwoing joint maximization:

$$\widehat{\mathbf{f}} = \arg\max_{\mathbf{f}} p(\mathbf{f}, \mathbf{g}|\mathbf{l}) \quad (17)$$

$$\widehat{\mathbf{l}} = \arg\max_{\mathbf{l}} p(\mathbf{f}, \boldsymbol{l}). \quad (18)$$

Maximization (17)-(18) is however equivalent to

$$(\widehat{\mathbf{f}}, \widehat{\mathbf{l}}) = \arg\max_{\mathbf{f},\mathbf{l}} p(\mathbf{f}, \mathbf{l}|\mathbf{g}) \quad (19)$$

whis is exactely the MAP solution associated to density $p(\mathbf{f}, \mathbf{l}|\mathbf{g})$.

Althouh we have followed a detection theory point of view, concerning image $\mathbf{l}$, the proposed methodoly can be casted into a Baysiean perspective. This stratagem will be fruitfull in the next solution when computing images $\widehat{\mathbf{f}}$ and $\widehat{\mathbf{l}}$.

IV. Computing the MAP solution

According to the rationale presented above, we have to determine

$$(\widehat{\mathbf{f}}, \widehat{\mathbf{l}})_{MAP} = \arg\max_{\mathbf{f},\mathbf{l}} p(\mathbf{f}, \mathbf{l}|\mathbf{g}). \quad (20)$$

Computing the MAP solution leads to a huge non-convex optimization problem, involving continous and discrete variables, with unbearable computation burden. Instead of determining exactly $(\widehat{\mathbf{f}}, \widehat{\mathbf{l}})_{MAP}$, we propose a continuation method which although not yielding the global maximum of $p(\mathbf{f}, \mathbf{l}|\mathbf{g})$, delivers nearly optimum estimates with a feasible computational load. Aiming at this goal, define

$$p(\mathbf{f}, \mathbf{l}|\mathbf{g}, \beta) = \frac{1}{Z(\beta)} e^{-\beta U(\mathbf{f},\mathbf{l}|\mathbf{g})}. \quad (21)$$

Under a statistical physical interpretation, parameter β is the inverse of the temperature ($\beta = 1/T$); this parameter controls the prominence of the maxima of (21): when

$\beta \to 0$, all configurations of $(\mathbf{f}, \mathbf{l})$ are equiprobable; when $\beta \to \infty$, the absolute maxima becomes progressively more marked, and in limit the set of the absolute maxima has probability one.

Annealing algorithms, of wich *mean field annealing* [6] (MFA) is an example, exploit this behaviour to establish continuation methods in which the temperature plays the role of continuation parameter.

The proposed continuation scheme evaluates, for an increasing sequence β_t, with $t = 1, \ldots, t_m$, the maximum $\widehat{\mathbf{f}}^{(t)}$ of $p(\mathbf{f}, \widehat{\mathbf{l}}^{(t-1)}|\mathbf{g})$, with respect to $\mathbf{f}$, follwed by the *mean line field* $\widehat{\mathbf{l}}^{(t)} = E_{\beta_t}[\mathbf{l}|\widehat{\mathbf{f}}^{(t)}, \mathbf{g}]$ (symbol E_β denotes the mean value operator computed according to density (21)). Based on this operation, we call the algorithm *expectation maximization annealing* (EMA).

EMA Algorithm

Initialization: set $\widehat{h}_{ij}^{(0)} = \widehat{v}_{ij}^{(0)} := 0.5$, $t = 1$, β_0, a, m

DO

step 1: $\widehat{\mathbf{f}}^{(t)} = \arg\max_{\mathbf{f}} p(\mathbf{f}, \widehat{\mathbf{l}}^{(t-1)}|\mathbf{g})$ (22)

step 2: $\widehat{\mathbf{l}}^{(t)} = E_{\beta_t}[\mathbf{l}|\widehat{\mathbf{f}}^{(t)}, \mathbf{g}]$ (23)

step 3: $\beta_{t+1} = a\beta_t$ (24)

While $t \leq m$

Due to the already pointed out behaviour of (21), it follows that

$$E_\beta[\mathbf{l}|\mathbf{f}, \mathbf{g}] \to \arg\max_{\mathbf{l}} p(\mathbf{f}, \mathbf{l}|\mathbf{g}), \qquad \beta \to \infty. \tag{25}$$

Therefore the stationaty points of the EMA algorithm are, at least, local maxima of $p(\mathbf{f}, \mathbf{l}|\mathbf{g})$; the *quality* of the maxima depends on the schedule of β_t.

Maximization (22) is implemented by the *iterated conditional modes* (ICM) method [17]. This is a coordinate-wise ascent technique, that maximizes the posterior distribution with respect to each individual component. After sweeping all image, the procedure is repeated until no noticiable energy increments are obtained.

The sationary points of (9), with respect to f_{ij}, are zeros of the fourth order polynomial

$$-4\mu\left((1-4\omega) + \omega(\bar{h}_{ij} + \bar{h}_{i+1,j} + \bar{v}_{ij} + \bar{v}_{i,j+1})\right) f_{ij}^4 + 4\mu\omega\bar{f}_{ij} f_{ij}^3 - 2M f_{ij}^2 + 2M g_{ij} = 0. \tag{26}$$

For each site (i, j) the solution of equation (26) is chosen to be the one root that maximizes $p(\mathbf{f}, \mathbf{g}|\mathbf{l})$.

Step (23) of the EMA algorithm is similar to the equivalent step of *mean field algoritm* (MFA); using the rationale proposed in [6], one obtains

$$v_{ij} := E_\beta[v_{ij}|\mathbf{f}, \mathbf{g}] \quad = \quad \frac{1}{1 + e^{2\mu\omega\beta\left\{\alpha - (\Delta_{i,j}^h)^2\right\}}} \tag{27}$$

A similar result is obtained for $\bar{h}_{ij} := E_\beta[h_{ij}|\mathbf{f}, \mathbf{g}]$, replacing h by v and vice versa in (27).

The EMA algorithm differs from the MFA in the step (23): while the latter evaluates mean value $E_{\beta_t}[\mathbf{f}|\widehat{\mathbf{l}}^{(t)}, \mathbf{g}]$, the former maximizes $p(\mathbf{f}, \widehat{\mathbf{l}}^{(t)}|\mathbf{g})$ with respect to $\mathbf{f}$. For Gaussian observation models both estimates are equal. This is not, however, the present case, since the obsevation model is not Gaussian.

Although not explicitly, function $p(\mathbf{f}, \mathbf{g}|\mathbf{l})$ depends on parameter μ. Since $Z_1(\mathbf{l}) \propto \mu^{-N^2/2}$, we obtain from (9) the ML estimate

$$\widehat{\mu}_{ML} = \frac{N^2}{4\sum_{ij} \omega\bar{v}_{ij}(\Delta_{ij}^h)^2 + \omega\bar{h}_{ij}(\Delta_{ij}^v)^2 + \frac{1}{2}(1-4\omega) f_{ij}^2}. \tag{28}$$

Therefore, if μ is unknown, it can be iteratively evaluated when implementing the EMA.

V. Experimental Results

In this section we present restoration results applied to real SAR data. The EMA algoritm is parametrized with $m = 10$ (number of temperature iterations), $a = 1.259$ (increasing rate of β), and $P_F = 10^{-3}$. Parameter μ is estimated according to (28).

Fig. 1(a) shows a SAR image of the agricultural landscape of Flevoland region in northern Netherlands. The image was acquired with 12.5m of pixel spacing and has four-looks. Part (b) displays the restored image with the line field superimposed. The EMA algorithm performs very well, as it can be perceived from the plot shown in part (c) of Fig. 1: the squared root of intensity data jointly with the restored image are plotted for column 300 (image has size 512×512). The algorithm correctly smoothes data within homogeneous regions, preserving discontinuities between neighboring regions. and Tiago Silva

VI. Concluding Remarks

A new restoration scheme for speckled images, acquired by coherent imaging systems, was presented. The knowledge of the statistics of the speckled images was fully taken into account through the observation model. The prior, a *compound Gauss Markov random field*, was used to tackle images exhibiting piecewise homogenous regions. A detection theoretical framework was adopted for locating the model discontinuities; more specifically, the Neyman-Pearson detection criterion was used, thus allowing to select a given false alarm probability in signaling discontinuities. A restoration of a real SAR image, suggests the adequacy of the proposed methodology.

Acknowledgment

The authors wishes to thank Dr. P. C. Smits, University of Genoa, for providing the SAR data.

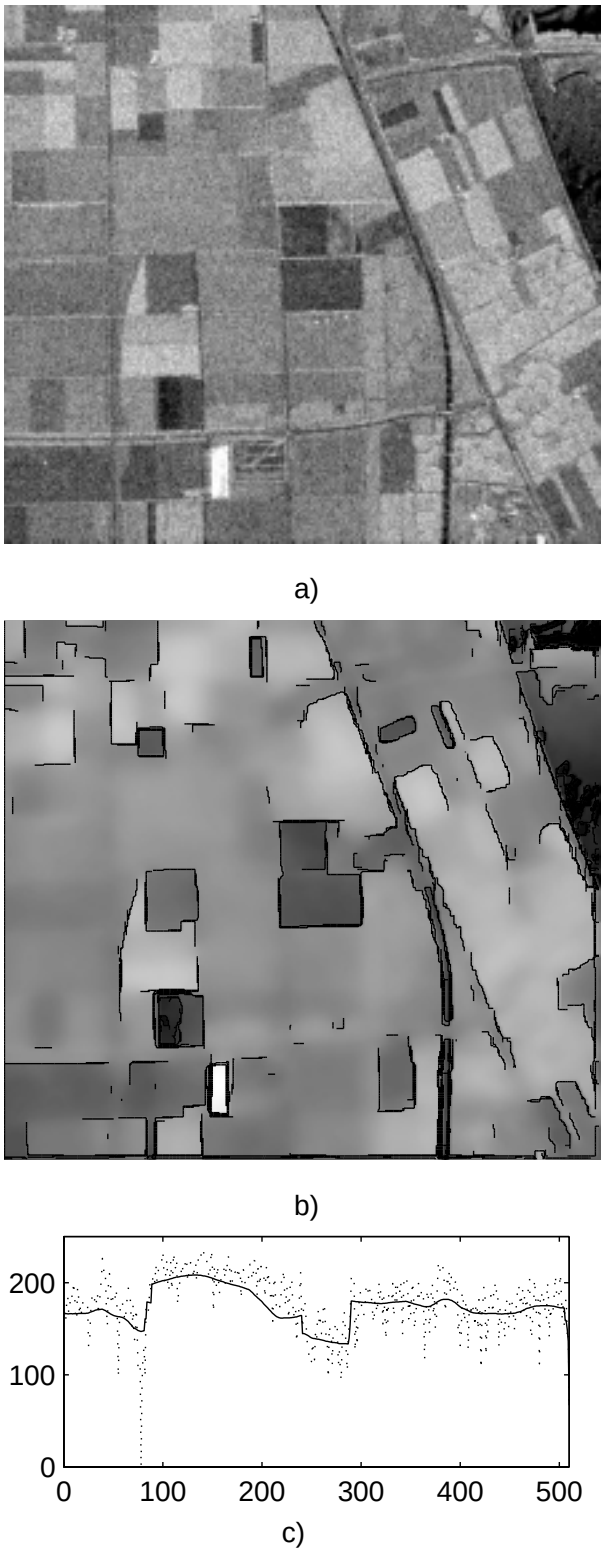

Fig. 1. SAR image of agricultural fields in the Flevoland, Netherlands: a) original image; b) estimated image considering $M = 4$ looks. The resulting segmentation is superimposed on both a) and b); estimated values along a straight line.

References

[1] S. Lowenthal and H. Arsenault, "Image formation for coherent diffuse objects: statistical properties", *J. Opt. Soc. Amer.*, vol. 60, pp. 1487–1493, Nov. 1970.

[2] J. Goodman, "Some fundamental properties of speckle", *J. Opt. Soc. Amer.*, vol. 66, pp. 1145–1150, Nov. 1976.

[3] H. Derin, P. Kelly, G. Vézina, and S. Labitt, "Modelling and segmentation of speckled images using complex data", *IEEE Trans. Geosci. Remote Sensing*, vol. 28, pp. 76–87, 1990.

[4] A. Blake and A. Zisserman, *Visual Reconstruction*, MIT Press, Cambridge, M.A., 1987.

[5] S. Geman and D. Geman, "Stochastic relaxation, Gibbs distribution and the Bayesian restoration of images", *IEEE Trans. Pattern Analysis and Machine Intelligence*, vol. PAMI-6, pp. 721–741, Nov. 1984.

[6] D. Geiger and F. Girosi, "Parallel and deterministic algorithms from MRF's: Surface reconstruction", *IEEE Trans. Pattern Analysis and Machine Intelligence*, vol. PAMI-13, pp. 401–412, May 1991.

[7] V. Frost, K. Shanmugan, and J. Holtzman, "A model for radar images and its applications to adaptive digital filtering of multiplicative noise", *IEEE Trans. on Pattern Analysis and Machine Intelligence*, vol. 2, pp. 157–166, 1982.

[8] D. Kuan, A. Sawchuk, T. Strand, and P. Chavel, "Adaptive restaration of images with speckle", *IEEE Trans. Acoust. Speech Signal Process.*, vol. 35, pp. 373–383, 1987.

[9] A. Bovik, "On detecting edges in speckle imagery", *IEEE Trans. Acoust. Speech Signal Process.*, vol. 36, pp. 1618–1627, 1988.

[10] P. Kelly, H. Derin, and K. Hartt, "Adaptive segmentation of speckled images using a hierarchical random field model", *IEEE Trans. Acoust. Speech Signal Process.*, vol. 38, pp. 1628–1641, 1988.

[11] E. Rignot and R. Chellapa, "Segmentation of polarimetric synthetic aperture radar data", *IEEE Trans. Image Process.*, vol. 1, pp. 281–300, 1992.

[12] A. Solberg, Torfinn Taxt, and A. Jain, "A Markov random field model for classification of multisource satellite imagery", *IEEE Trans. Geosci. Remote Sensing*, vol. 34, pp. 100–113, 1996.

[13] P. Smits and S. Dellepiane, "Discontinuity adaptive MRF model for remote sensing image analysis", *in IEEE International Geoscience and Remote Sensing Symposium-IGARSS'97*, vol. II, pp. 907–909, Singapore, August 1997.

[14] F. Jeng and J. Woods, "Compound Gauss-Markov random fields for image processing", in A.Katsaggelos, editor, *Digital Image Restoration*, pp. 89–108. Springer Verlag, 1991.

[15] J. Dias, T. Silva, and J. Leitão, "Adaptive restoration of speckled SAR images", *in IEEE International Geoscience and Remote Sensing Symposium- IGARSS'98*, Seattle, July 1998.

[16] R. Touzi, A. Lopes, and P. Bousquet, "A statistical and geometrical edge detector for sar images", *IEEE Trans. Geosci. Remote Sensing*, vol. 26, pp. 764–773, 1988.

[17] J. Besag, "On the statistical analysis of dirty pictures", *Journal of the Royal Statistical Society B*, vol. 48, pp. 259–302, 1986.

[18] M. Figueiredo and L. Leitão, "Unsupervised image restoration and edge location using compound Gauss-Markov random fiels and the MDL principle", *IEEE Trans. Image Processing*, vol. 6, pp. 1089–1102, August 1997.

[19] H. V. Trees, *Detection, Estimation and Modulation Theory*, vol. I, John Wiley, New York, 1968.